



City Research Online

City, University of London Institutional Repository

Citation: Allen, A., Moulard, J. W., Rodgers, J., Bano-Otalora, B., Douglas, R. H., Jeffery, G., Vugler, A. A., Brown, T. M. & Lucas, R. J. (2020). The spectral sensitivity of cone vision in the diurnal murid, *Rhabdomys pumilio*. *The Journal of Experimental Biology*, 223(11), jeb215368. doi: 10.1242/jeb.215368

This is the published version of the paper.

This version of the publication may differ from the final published version.

Permanent repository link: <https://openaccess.city.ac.uk/id/eprint/24077/>

Link to published version: <https://doi.org/10.1242/jeb.215368>

Copyright: City Research Online aims to make research outputs of City, University of London available to a wider audience. Copyright and Moral Rights remain with the author(s) and/or copyright holders. URLs from City Research Online may be freely distributed and linked to.

Reuse: Copies of full items can be used for personal research or study, educational, or not-for-profit purposes without prior permission or charge. Provided that the authors, title and full bibliographic details are credited, a hyperlink and/or URL is given for the original metadata page and the content is not changed in any way.

City Research Online:

<http://openaccess.city.ac.uk/>

publications@city.ac.uk



City Research Online

City, University of London Institutional Repository

Citation: Allen, A., Mouland, J. W., Rodgers, J., Bano-Otalora, B., Douglas, R. H. ORCID: 0000-0002-6862-2768, Jeffery, G., Vugler, A. A., Brown, T. M. and Lucas, R. J. (2020). The spectral sensitivity of cone vision in the diurnal murid, *Rhabdomys pumilio*. *The Journal of Experimental Biology*, doi: 10.1242/jeb.215368

This is the accepted version of the paper.

This version of the publication may differ from the final published version.

Permanent repository link: <https://openaccess.city.ac.uk/id/eprint/24077/>

Link to published version: <http://dx.doi.org/10.1242/jeb.215368>

Copyright and reuse: City Research Online aims to make research outputs of City, University of London available to a wider audience. Copyright and Moral Rights remain with the author(s) and/or copyright holders. URLs from City Research Online may be freely distributed and linked to.

City Research Online:

<http://openaccess.city.ac.uk/>

publications@city.ac.uk

The spectral sensitivity of cone vision in the diurnal murid, *Rhabdomys pumilio*

Annette E Allen¹, Joshua W. Mouland², Jessica Rodgers¹, Beatriz Baño-Otálora¹, Ronald H. Douglas³, Glen Jeffery⁴, Anthony A Vugler⁴, Timothy M Brown², Robert J Lucas¹

1. Division of Neuroscience and Experimental Psychology, Faculty of Biology Medicine and Health, University of Manchester, UK.
2. Division of Diabetes, Endocrinology and Gastroenterology, Faculty of Biology Medicine and Health, University of Manchester, UK.
3. Department of Optometry and Visual Science, City, University of London, UK.
4. Institute of Ophthalmology, University College London, UK.

Abstract

An animal's temporal niche – the time of day at which it is active – is known to drive a variety of adaptations in the visual system. This includes variations in the topography, spectral sensitivity and density of retinal photoreceptors, and changes in the eye's gross anatomy and spectral transmission characteristics. We have characterised visual spectral sensitivity in the murid rodent *Rhabdomys pumilio* ('the four-striped grass mouse'), which is the same family as (nocturnal) mice and rats, but exhibits a strong diurnal niche. As is common in diurnal species, the *Rhabdomys* lens acts as a long-pass spectral filter, providing limited transmission of light <400nm. Conversely, we found strong sequence homologies with the *Rhabdomys* SWS and MWS opsins and those of related nocturnal species (mice and rats) whose SWS opsins are maximally sensitive in the near UV. We continued to assess *in vivo* spectral sensitivity of cone vision using electroretinography and multi-channel recordings from the visual thalamus. These revealed that responses across the human visible range could be adequately described by those of a single pigment (assumed to be MWS opsin) maximally sensitive ~500nm, but that sensitivity in the near UV required inclusion of a second pigment whose peak sensitivity lay well into the UV range (λ_{\max} <400nm, likely ~360nm). We therefore conclude that, despite the UV-filtering effects of the lens, the *Rhabdomys* retains an SWS pigment with a UV-A λ_{\max} . In effect, this somewhat paradoxical combination of long-pass lens and UV-A λ_{\max} results in narrow-band sensitivity for SWS cone pathways in the UV-A range.

Introduction

The vast majority of mammalian retinas contain three classes of photoreceptor: the outer-retinal rods and cones, that mediate form vision in dim and bright conditions, respectively; and the inner-retinal intrinsically-photosensitive retinal ganglion cells (ipRGCs), which contribute a lower spatiotemporal resolution representation of the visual environment supporting aspects of vision as well as an array of non-image forming light responses (e.g. photoentrainment of the circadian clock). Collectively, these photoreceptors allow organisms to sense and respond to light across the broad variations in illumination that they would commonly encounter in the natural world. Nevertheless, striking variations in mammalian photoreception have emerged throughout evolution, and the spectral sensitivity, anatomical distribution, and relative number of each photoreceptor type can vary greatly amongst species (Peichl 2005). In many cases, this can be attributed to a shift in a species' temporal niche (the time of day at which an animal is most likely to be active), which defines both the quality and quantity of environmental light exposure an animal experiences day to day.

Whether diurnal or nocturnal, most mammalian retinas contain two classes of cone photoreceptor, that are preferentially sensitive to different spectral bands owing to their expression of either short or medium/long-wavelength sensitive photopigments (SWS and MWS, respectively (Jacobs 1993)). Within these classes, there are substantial species differences in spectral sensitivity (Jacobs 1993, Hunt et al. 2009). There is some evidence to suggest that, at least for SWS pigments, a diurnal temporal niche is associated with a shift in spectral sensitivity towards longer wavelengths (from λ_{\max} = 350-370nm in nocturnals to λ_{\max} >400nm in diurnals; (Emerling et al. 2015)). By comparison, the spectral tuning of rod

pigments remains largely invariant amongst terrestrial mammals, with λ_{\max} values remaining close to 500nm. As well as the spectral tuning of the visual pigments, pre-receptor filtering by the lens constrains the spectral sensitivity of mammalian vision (Douglas and Jeffery 2014), and is strongly associated with temporal niche. Nocturnal species' lenses typically transmit the majority of UV-A light (~315-400nm), while day-dwelling mammals have a 'long-pass' lens which prevents transmission of shorter wavelength light. Indeed, this filtering property can be used as a good predictor of species' temporal niche (Hut et al. 2012). It is thought that limiting UV-A transmission in diurnal species could serve to reduce damage from UV light (van Norren and Gorgels 2011) and/or to aid higher acuity vision in diurnal species by minimising the impact of chromatic aberration; (Lind et al. 2014) and reducing the amount of Rayleigh scatter (Douglas and Jeffery 2014). The density of cone photoreceptors across the retina also shows dramatic shifts in nocturnal vs. diurnal species (Hut et al. 2012), with the latter classically having a greater cone density to match their increased exposure to bright light. Sometimes that increased density is apparent across the entire retina (such as in the thirteen-lined ground squirrel (Kryger et al. 1998)), but it may also occur in spatially localised regions, such as the primate fovea (reviewed by Ahnelt and Kolb 2000).

Here, we ask whether these general rules hold for a murid rodent - *Rhabdomys pumilio* ('the four striped grass mouse') – which is closely related to (nocturnal) mice and rats, but exhibits a strong diurnal niche (Dewsbury and Dawson 1979, Schumann et al. 2005, Schumann et al. 2006). The *Rhabdomys* visual system shows several adaptations that are consistent with a diurnal niche, including an increased cone:rod ratio and high cone density (van der Merwe et al. 2018). However, the question of whether the visual system of *Rhabdomys* has 'diurnal' type spectral sensitivity remains outstanding. Here we find that, consistent with its diurnal niche, the *Rhabdomys* retina is cone-rich, and its lens transmits little UV light. On the other hand, electrophysiological recordings indicate that *Rhabdomys* SWS and MWS cones likely have surprisingly similar spectral sensitivities (predicted $\lambda_{\max} \approx 360\text{nm}$ and 500nm) to their closely related nocturnal counterparts. The outcome is that *Rhabdomys* spectral sensitivity is biased against UV-A wavelengths thanks to lens filtering, but not cone spectral sensitivity.

Materials and Methods

Animals

Animal care was in accordance with the UK Animals, Scientific Procedures Act of 1986, and the study was approved by the University of Manchester ethics committee. Animals were housed in 12:12 light-dark cycle at 22°C with food and water available ad libitum. All experiments were performed in adult *Rhabdomys* (aged 3-8 months).

RNA extraction and sequencing

Primer design: Primers were designed to amplify the first and last 100-200bp of SWS and MWS cone opsins from genomic DNA (gDNA). These primers were based on conserved regions of the mouse (*Mus musculus*) and rat (*Rattus norvegicus*) SWS and MWS sequences, genes obtained from NCBI Genbank (Gene IDs: 12057 mouse SWS; 14539 mouse MWS; 81644 rat SWS and 89810 rat MWS). Based on gDNA PCR sequencing results, subsequent primers were designed for cloning full-length coding sequence of *Rhabdomys* SWS and MWS cone opsin from retinal cDNA. Each primer included an additional overlapping sequence to allow cloning of full-length sequence into a linearised plasmid vector using Gibson assembly (Gibson et al. 2009).

Genomic DNA PCR: Genomic DNA was obtained from *Rhabdomys* ear biopsies. Genomic DNA PCR was performed using Q5 High-Fidelity DNA polymerase (NEB) according to manufacturer's instructions. The PCR products were run on a 1.5% agarose gel, gel extraction using QIAQuick Gel extraction (Qiagen) performed on any bands of expected/appropriate size and sequenced using Sanger sequencing.

Retina RNA Extraction and cDNA synthesis: *Rhabdomys* were culled, and both eyes removed and placed in cold sterile PBS. Each retina was then dissected and placed into a separate

sterile RNase and DNase free 1.5ml tube containing 0.5ml of RNAlater and placed on ice. Retina tissue was stored in RNAlater at -20°C until extraction RNA extraction was performed using RNeasy Mini Kit (Qiagen) according to manufacturer's instructions with additional on-column DNase digest (Qiagen) to eliminate potential genomic DNA contamination. Tissue was disrupted using mortar and pestle and homogenized with syringe and needle. The optional extra-elution step was also undertaken. RNA was immediately used for cDNA synthesis or stored at -80°C. cDNA synthesis was performed using qScript cDNA Synthesis Kit (QuantaBio) according to manufacturer's instruction, and stored at -20°C until use.

Cloning full-length cone opsin coding sequences: PCR of full length cone opsin coding sequences was performed on *Rhabdomys* retinal cDNA using Q5 High-Fidelity DNA polymerase (NEB; according to manufacturer's instructions). The following primers were used for SWS (forward 5' – ACTTAAGCTTCACCATGTCTGGGAGAGGACGAGT and reverse 5' – TCGAGCGGCCGCTTAGTGAGGGCCAACTTTGCT) and MWS (forward 5' – ACTTAAGCTTCACCATGGCCCAAAGGCTTACAGGT and reverse 5' – TCGAGCGGCCGCTTATGCAGGTGACACTGAAG). PCR products were run on a 1.5% agarose gel, and suitable-sized bands were removed and gel extracted using QIAquick Gel Extraction Kit (Qiagen). These were then cloned into pcDNA3 plasmid vector linearised with *HindIII* and *NotI* restriction enzymes using NEB HiFi DNA assembly according to manufacturer's instructions. 3µl of cloning reaction was then transformed in XL10 Gold cells (Agilent) and plasmid prepared using Qiaprep Spin miniprep kit (Qiagen). Full-length coding sequence of *Rhabdomys* SWS and MWS cone opsin was confirmed by Sanger sequencing of plasmid insert using following primers (CMV Fwd 5' – GGAGGTCTATATAAGCAGAGC and BGH Rev 5' – GGCACCTTCCAGGGTCAAGG).

Immunohistochemistry

Rhabdomys were perfused with 4% paraformaldehyde (methanol free). Eyes were then stored in methanol-free 4% paraformaldehyde prior to further processing. For retinal wholemounts, retinas were dissected from fixed eyes and immunohistochemistry performed on free-floating retinas. For retinal sections, whole eyes were embedded in Histo-resin and were sectioned at 5µm thickness. For general histology, fixed eyes were dehydrated through a graded series of alcohols and infiltrated with Technovit 7100 (Histo-resin TAAB Labs UK). Blocks were sectioned at 5µm and mounted onto clean slides and stained with cresyl violet and coverslipped under DPX. For immunohistochemistry, *Rhabdomys* retinas were labelled using polyclonal antibodies against MWS/LWS opsin raised in chicken: (PA1-9517; ThermoFisher; 1:250) and against SWS opsin raised in rabbit (AB5407, Abcam; 1:300), and left overnight at room temperature. Tissues were then washed and incubated for 2 hours in fluorescent secondary antibodies at a dilution of 1:2000 made up of 2% NDS, 3% Triton X-100, and PBS. Sections were imaged with Axio Imager.D2 upright microscope and captured using a Coolsnap Hq2 camera (Photometrics) through Micromanager software v1.4.23.

Lens transmission

Lens transmission was assessed as described previously (Douglas and Jeffery 2014). Briefly, *Rhabdomys* were culled and both eyes removed. Lenses were dissected and immediately frozen (n = 5 lenses from 3 female *Rhabdomys*). After thawing, lenses were rinsed in phosphate-buffered saline (PBS) and mounted in a purpose built holder in front of an integrating sphere, within a Shimadzu 2101 UVPC spectrophotometer. Transmission at 700nm was set to 100%, and lenses scanned at 1nm intervals from 300-700nm. An equivalent procedure was used to calculate the transmission from n=16 mouse eyes.

Electroretinography

Electroretinograms (ERGs) were recorded from 6 *Rhabdomys* (4 female, 2 male), using apparatus and methodology as described previously (Cameron and Lucas 2009). Anaesthesia was induced with isoflurane (2% in Oxygen), and maintained with an intraperitoneal injection of Urethane (1.6g/kg, 30% w/v; Sigma-Aldrich, UK). A topical midriatic (tropicamide 1%;

Chauvin Pharmaceuticals, Surrey, UK) and hypromellose eye drops were applied to the recording eye prior to placement of a corneal contact lens-type electrode (Sagdullaev et al. 2004). A needle reference electrode was inserted approximately 5mm from the base of the contralateral eye, and a bite-bar was used for head support and also acted as a ground electrode. Electrodes were connected to a Windows PC via a signal conditioner (model 1902 Mark III, Cambridge Electronic Design, UK) that differentially amplified and filtered (band-pass filter cut-off 0.5-200Hz) the signal, and a digitiser (model 1401, Cambridge Electronic Design, UK). Core body temperature was maintained at 37°C throughout recordings via a homeothermic heat mat (Harvard Apparatus, UK).

Visual stimuli: ERG

A CoolLED pe-4000 was used to present 13 stimuli of distinct spectra, with peak wavelengths ranging from 365 – 660nm. The output was passed through a filter wheel containing a range of neutral density filters, which allowed the light to be modulated across a 6 log unit range. The intensities of each channel were made approximately isoquantal by adjusting the absolute power of each LED, and by using an Arduino Uno to further adjust the PWM of each channel on an 8 bit scale. Stimuli were measured at the corneal plane using a spectroradiometer (SpectroCAL MSII, Cambridge Research Systems, UK). All stimuli used were quantified in terms of their photon flux, after accounting for the spectral transmission of the *Rhabdomys* lens.

Stimuli were presented following 30 minutes dark adaptation. Stimuli of different spectra were presented in a pseudorandom order, at 6 intensity levels (moving from dim to bright using a neutral density filter wheel). Dark adapted stimuli were either presented as a flash (10ms every 1s); or as a 32Hz flicker. Stimuli were also presented at a range of frequencies (1-50Hz), using a broadband white quartz halogen light (8.6×10^{15} photons/cm²/s) coupled to a mechanical shutter to modulate stimulus frequency. Spectral stimuli were also measured in light-adapted conditions, whereby the filtered output of a quartz halogen light source (500nm short-pass filter; 4.6×10^{14} photons/cm²/s) was superimposed upon narrowband spectra. Stimuli were combined using a bifurcated mixed fibre optic with opal diffuser at the output.

A further set of stimuli were designed using the principles of receptor silent substitution (as used previously, (Allen et al. 2014, Allen and Lucas 2016)). Briefly, a pair of spectra were generated using a combinations of CoolLED channels, which were designed to be isoluminant for *Rhabdomys* MWS and SWS opsins (using putative λ_{maxes} of 360nm and 500nm; stimuli nominally termed 'stimulus' and 'background' spectra). A second pair of spectra was generated, designed to be isoluminant for *Rhabdomys* MWS opsin but present 99% Michelson contrast for the putative *Rhabdomys* SWS opsin. ERGs were then recorded whilst transitions between these pairs of spectra were presented to the *Rhabdomys* eye (10ms flash of 'stimulus' spectrum interleaved with 990ms of 'background' spectrum).

For flash ERGs, b-wave amplitudes were measured relative to the baseline (value at flash onset) or, when measurable, relative to the trough of the preceding a-wave. For all flicker ERGs, a mean of each 1s-cycle was taken; the average amplitude of the first 4 peak to trough responses was measured, with a period equal the stimulus frequency.

In vivo electrophysiological recordings in LGN

In vivo electrophysiological recordings were performed in 3 *Rhabdomys*, using methods as described previously (Brown et al. 2012). Anaesthesia was induced with 2% isoflurane in oxygen, and maintained with an intraperitoneal injection of urethane (1.6g/kg, 30% w/v; Sigma-Aldrich, UK). A topical mydriatic (as with ERGs) and mineral oil (Sigma-Aldrich, UK) were applied to the left eye prior to recording. After placement into a stereotaxic frame, the *Rhabdomys*' skull was exposed and a small hole drilled ~2.5mm posterior and ~2.5mm lateral to bregma. A 256-channel recording probe (A4x64-Poly2-5mm-23s-250-177-S256; NeuroNexus Technologies, Inc., MI, USA) consisting of 4 shanks spaced 200µm apart, each with 64 recording sites, was lowered a depth of ~3-3.5mm into the brain, targeting the

Rhabdomys LGN. Broadband neural signals were then acquired using a SmartBox recording system (NeuroNexus Technologies, Inc., MI, USA), sampling at 20kHz. Following recordings, data from each of the four electrode shanks was pre-processed by common median referencing, high pass filtered at 250Hz and then passed to an automated template-matching-based algorithm for single unit isolation (Kilosort; (Pachitariu et al. 2016)). Isolated units were then extracted as virtual tetrode waveforms for validation in Offline Sorter (V3, Plexon, TX, USA). Here, unit isolation was confirmed by reference to MANOVA F statistics, J3 and Davies-Bouldin validity metrics and the presence of a distinct refractory period (greater than 1.5 ms) in the interspike interval distribution.

Spike sorted data were further analysed in MATLAB R2018a (The Mathworks). Perievent response histograms for each stimulus were calculated (250ms bins; mean of 20 trials) with response quantified as the maximum absolute change in spike rate during or in the 1s following visual stimulation relative the baseline (mean spike rate in the 1s prior to visual stimulation). This approach therefore captured both ON and OFF responses. To identify significant changes in spike rate, responses calculated in this manner were compared to the distribution of 'response' values determined from 1000 repeats using trialxtrial time-shuffled spike counts. The mean of the shuffled response distribution was subsequently subtracted from the actual response such that, on average, a lack of response would give a value of 0 spikes/s.

Visual stimuli: LGN

Experiments employed a custom built light source (all components from Thorlabs, Ely, UK) consisting of a cold white LED (MCWHLP1) with an automated narrowband filter wheel (FW102C, loaded with bandpass filters at 425, 450, 495, 530, 560 and 600nm; bandwidth: ± 10 nm) and a second adapting cold white LED fitted with selectable blue and yellow broadband filters (centred at 450 and 550nm respectively; bandwidth: ± 40 nm). LED intensity was controlled by current modulation via T-Cube drivers and, where required, neutral density filters. Output from the adapting and probe sources was then combined and delivered to the subject via a randomised bifurcated light guide (E436, Dolan Jenner, MA, USA) whose output ferrule (6.3mm diam.) was positioned 5mm from the contralateral eye and enclosed by an internally reflective plastic cone to provide approximately full field illumination. Stimulus measurements were performed using a calibrated spectroradiometer as above.

Stimulus delivery was controlled using LabVIEW (National Instruments, TX, USA). Animals were first dark adapted for 30 mins. To assess rod spectral sensitivity we delivered dim 1s narrowband flashes across the six available test wavelengths at six different intensities ($\sim 10^8$ - $10^{10.5}$ photons/cm²/s; 20 repeats per intensity/wavelength). The order of stimulus delivery was randomised according to wavelength between each of the 20 trials but scheduled such that lowest intensity trials were completed first and highest intensities last. Subsequent assessment of cone spectral sensitivity was performed similarly except in this case we employed seven rather than six intensities at each wavelength ($\sim 10^{12}$ - $10^{14.5}$ photons/cm²/s) and stimuli were superimposed on a rod-saturating short followed by long wavelength background ($\sim 10^{13.5}$ rod effective photons/cm²/s for both).

Note that a different set of spectral stimuli were used with dLGN and ERG experiments, owing to technical constraints. Nevertheless, our experiments were carefully designed with this constraint in mind. Thus, while our ERG studies provide the comprehensive description of sensitivity across a wide wavelength range, our dLGN experiments were designed to determine whether: 1.) *Rhabdomys* use a dedicated short wavelength sensitive receptor (revealed by the presence of neurones responsive to short but not longer wavelength stimuli); and 2.) the SWS cone has λ_{\max} in the UV range, by determining whether responses to shorter wavelength stimuli survive application of a background that should suppress responses from any pigment with peak sensitivity >400 nm.

Analysis of spectral stimuli

All spectral stimuli used were quantified in terms of their absolute photon flux, as described previously (Allen et al. 2014). Two approaches were used to predict the spectral sensitivity of *Rhabdomys* cone opsins from ERG studies. First, irradiance response functions were plotted for each wavelength, and data fitted with a sigmoidal dose response curve: $Y = a + (b-a)/(1+10^{(\text{LogEC50-X})})$, where a = base and b = top of curve. For wavelengths that evoked responses at only one or two intensities, data were not included due to ambiguous curve fits. Curve parameters were fixed across each stimulus, such that the only free parameter was the EC50. EC50 values were then plotted as a function of wavelength. Note, however, that bandwidth was often >25nm (FWHM), and hence when plotting response amplitude as a function of wavelength, the peak wavelength of each channel was used. The best fitting λ_{max} was calculated using a Govardovskii nomogram (Govardovskii et al. 2000).

In a second approach, we modelled the sensitivity of two hypothetical cone opsins to find the combination of λ_{max} values that best described physiological responses. First, we calculated the predicted photon fluxes of SWS and MWS opsins with a range of hypothetical λ_{max} values (ranging from 360-420 and 470-530nm, respectively), and with a range of weighted contributions, using the following formula:

$$\text{Effective photon flux} = \int P(\lambda) \cdot ((s_A(\lambda) \cdot k_A) + (s_B(\lambda) \cdot k_B)) \cdot I(\lambda) d\lambda,$$

where $P(\lambda)$ is spectral irradiance in photons per square centimetre per seconds per nanometre, $s_A(\lambda)$ and $s_B(\lambda)$ are pigment spectral sensitivity approximated by the Govardovskii visual template (for two pigments, 'A' and 'B', incorporating a beta peak; (Govardovskii et al. 2000)), k_A and k_B are relative weighting factor (for pigments A and B), and $I(\lambda)$ is *Rhabdomys* lens transmission.

For each combination, we plotted the response at each intensity at each wavelength as a function of effective rate of photon flux for a weighted combination of the two hypothetical pigments. We then tested which combination of λ_{max} and weighted contribution to the evoked response allowed the combined intensity response curve to be best fit by a single curve.

For LGN recordings, we used a qualitatively equivalent (but computationally faster) approach to estimate single cell spectral sensitivity. Hence, here spectral sensitivity was determined by calculating irradiance response relationships across all test wavelengths according to the effective photon flux experienced by a single opsin with arbitrary λ_{max} in the range 350-600nm (taking into account *Rhabdomys* lens transmission). We then calculated the four-parameter sigmoid curve that best fit that irradiance response relationship and determined the %variance in the data accounted for by that fit. Analysis of a subset of cells using the first approach described above for ERG produced identical λ_{max} estimates.

To add context to the transmission characteristics of the *Rhabdomys* lens, we calculated the impact of the lens transmission on the effective photon flux of *Rhabdomys* and mouse SWS and MWS pigments in natural daylight (using spectra measured in Manchester, UK (53°21' N, 2°16' W, elevation of 78m), 2 weeks after Summer solstice, at a solar angle of +30° (published previously (Allen et al. 2014))).

Results

Rhabdomys SWS and MWS-cone opsins

We were able to amplify full-length sequences for both SWS and MWS cone opsins from *Rhabdomys* retinal cDNA (Fig 1). The predicted sequences for these two opsins are 346 and 359 amino acids long, respectively. When aligned against the corresponding opsin sequence from multiple other rodent species (*Mus musculus* (mouse), *Rattus norvegicus* (rat), *Octodon degus* (degu), *Meriones unguiculatus* (gerbil), *Ictidomys tridecemlineatus* (thirteen-lined ground squirrel) and *Cavia porcellus* (guinea pig)), *Rhabdomys* opsins showed highest sequence homology with mouse and rat, (~96% and 97% respectively) as predicted for the

phylogeny of these species (Blanga-Kanfi et al. 2009) (sequence homologies are summarised in table 1).

A high degree of homology was retained at known spectral tuning sites between cone opsins of *Rhabdomys* and other rodent species. The *Rhabdomys* cone opsin sequences had highly conserved opsin characteristics, such as the chromophore binding site, Lys296, and retinal counter-ion, Glu113 (numbering throughout based on bovine rod opsin). When we examined known spectral tuning sites, we found the *Rhabdomys* sequences were most similar to rats and mice. For example, *Rhabdomys*, mice and rats all possessed phenylalanine at position 86, which has been established as an important site for UV spectral tuning in vertebrates (Cowing et al. 2002, Fasick et al. 2002, Hunt et al. 2004, Hunt et al. 2007). When we examined MWS opsin sequences at the “five-sites” involved in spectral tuning differences between MWS/LWS photopigments (Yokoyama and Radlwimmer 1998), we found these residues in *Rhabdomys* cone opsin were identical to rat and mouse sequences (Ala164, Tyr181, Glu261, Tyr269, and Ser292, respectively). Initial analysis of the predicted protein sequence suggests spectral tuning of *Rhabdomys* cone opsins may be similar to that of rat or mouse.

Immunohistochemical labelling of cone opsins in the *Rhabdomys* retina identified both SWS and MWS expressing cones (Fig 2a). Unlike in mice (Applebury et al. 2000), we saw no evidence of cones co-expressing both types of opsin. A recent analysis of cone densities in the *Rhabdomys* retina (van der Merwe et al. 2018) reported that MWS expressing cones were more numerous than SWS cones across the retina, and that both cones showed lower density in the periphery. We did not undertake an extensive validation of those observations, but our immunocytochemistry did confirm that MWS cones were substantially more numerous than SWS cones (Fig 2a).

Spectral transmission of Rhabdomys lens.

As a prelude to descriptions of *Rhabdomys*' spectral sensitivity *in vivo*, we measured spectral transmission of the *Rhabdomys* lens across the UV-visible wavelength range (5 adult *Rhabdomys* lenses; mean diameter along the optic axis 2.6mm; Fig 2b). We found that the *Rhabdomys* lens acts as a long pass filter, allowing efficient transmission of wavelengths $\geq 400\text{nm}$ (50% transmission at $383.5\text{nm} \pm 1.2\text{nm}$; Fig 2c). The *Rhabdomys* lens is therefore substantially less transmissive for UV light than mouse or rat lenses, both of which have a 50% transmission point at a wavelength approximately 70nm shorter (Douglas and Jeffery 2014).

Rhabdomys in vivo spectral sensitivity – ERG

We continued to assess the spectral sensitivity of *Rhabdomys* vision using the electroretinogram (ERG). To begin, we established the basic temporal response characteristics of the *Rhabdomys* ERG by recording dark-adapted responses to full-field flicker across a range of frequencies (ranging from 1-50Hz; 100% contrast). In such conditions, ERGs were measurable at frequencies $\leq 40\text{Hz}$ (Fig 3a&b). Mice and rats are able to track flicker up to a similar frequency when measured in cone-isolating (light-adapted) conditions (Krishna et al. 2002, Qian et al. 2008). Across this frequency range, under these conditions, one would expect a switch from rod + cone towards predominantly cone-based responses. We therefore recorded ERG spectral sensitivity at low and high temporal frequencies (1 and 32Hz) by recording responses to 13 spectrally distinct (~isoquantal) stimuli across a 6-log unit range of light intensities (Fig 3c). When presented at 1Hz, we were able to record measurable ERGs to the brightest flash across all wavelengths (Fig 3d). Irradiance response curves revealed maximum sensitivity around 500nm (Fig 3e), which would be typical for a rod-driven response across other mammalian species. However, when we quantified relative sensitivity across wavelengths, we found higher sensitivity to the shortest wavelength tested than predicted for a single photopigment with λ_{max} around 500nm when accounting for pre-receptor filtering by the *Rhabdomys* lens (Fig 3f). The simplest explanation is that there is some intrusion of SWS-cones to this response. We therefore asked whether inclusion of an additional short wavelength pigment improved the fit of the data. Given that intensity response

functions had a qualitatively similar form across the wavelength range (Fig 3e) we applied a simple modelling process in which we asked what combination of pigments would be required to predict the pattern of relative sensitivity across wavelengths. In brief, we attempted to describe measured sensitivity across all wavelengths by calculating an effective photon flux for a system in which responses were elicited by the combined activity of two opsin pigments with different spectral sensitivity. To achieve the objective of having the same response to a given effective photon flux irrespective of wavelengths we varied three parameters: the peak sensitivity (λ_{\max}) of each opsin, and their relative contribution to the evoked response for a theoretical spectrally neutral light source (contribution weighting ratio). This method achieved a good fit for the data using pigments with predicted λ_{\max} 360 and 504nm at 1:6 contribution weighting (Fig 3g). The predicted spectral sensitivity function for this combination of opsins, and accounting for the filtering effects of the lens, is shown in Fig 3h.

The appearance of a short wavelength cone component to the 1Hz response might have been expected given the cone rich nature of the *Rhabdomys* retina. More surprising was that there was no requirement to account for an additional MWS-cone contribution to the response. The most likely explanation is that the MWS opsin has maximal sensitivity around 500nm, near peak sensitivity of the 1Hz response. Extending our spectral sensitivity investigation to conditions favouring cones (32Hz flicker) confirmed that this is indeed the case (Fig 4a&b). Once again, responses could be recorded across the wavelength range and peak sensitivity lay around 500nm (Fig 4c). Applying the same criteria used for 1Hz responses revealed that the data could be adequately fit by a 1:4 combination of opsins with λ_{\max} 360 and 500nm (Fig 4d-e). The prediction that MWS opsin has a greater impact on flicker spectral sensitivity than SWS opsin is consistent with our own (Fig 2) and published (van der Merwe et al. 2018) observations that MWS cones are more numerous in the *Rhabdomys* retina. The reduction in this ratio compared to that recorded at 1Hz (at which it is 1:6; Fig 3g) likely reflects the additional contribution of rods to middle/long wavelength sensitivity at low temporal frequencies.

As a further confirmation that the high frequency flicker stimuli faithfully reported cone visual sensitivity, we repeated those recordings under light adapted conditions with the goal of saturating any residual rod-evoked responses. We recorded flicker ERG responses following adaptation to (and in the presence of) a broad-spectrum background light covering the spectral sensitivity range expected for rods and the two putative cone pigments (Fig 5). The background light had no discernible impact on flicker ERG spectral sensitivity. Thus, modelling the data as the output of a combination of two pigments (as above), returned λ_{\max} of 360 and 503nm. Note that the adapting light is predicted to differentially impact middle/long wavelength pigments, which likely explains the increase in contribution weighting of SWS vs MWS opsins to 1:10 for this high frequency flicker stimulus compared to that recorded under dark adapted conditions.

As lens filtering of UV light makes it difficult to unambiguously record a short wavelength peak in the composite ERG attributable to SWS-cones, we set out to use the approach of receptor silent substitution to record an isolated SWS response. First, we generated a pair of spectrally distinct stimuli that were designed to be isoluminant for these two proposed photopigments (<5% Michelson contrast). In accordance with our prediction, transitions between these two spectra (10ms/1000ms) drove no measurable ERG response (Fig 6a&b). We then designed a pair of stimuli that were isoluminant for putative MWS-cones, but presented contrast for an SWS pigment. Transitions between these spectra elicited a flash ERG response (Fig 6c&d). This confirms that the *Rhabdomys* ERG cannot be accounted for by a single pigment with λ_{\max} around 500nm.

Rhabdomys in vivo spectral sensitivity – dLGN

Our ERG data describe the spectral sensitivity of *Rhabdomys* cone visual responses, but the lens filtering of UV light makes the contribution of SWS opsin to the composite spectral sensitivity profile slight. As additional confirmation that there was indeed an independent short

wavelength sensitive contribution to visual responses we turned to recordings in the dLGN, in which a subset of individual units might reasonably be expected to convey information only from SWS cones. To this end, we performed large scale multielectrode recordings from the *Rhabdomys* lateral geniculate nucleus (LGN; 256-channel recordings from 3 *Rhabdomys*). Using this approach, we were able to describe the spectral sensitivity of individual neurons, as opposed to a composite response, and therefore test the prediction that some neurons would exhibit specific short-wavelength sensitivity in the UV range.

To determine the functional spectral sensitivity of the isolated neurons, we presented a series of 6 spectrally distinct stimuli (randomised order) as 1s full field flashes across a ~2 log unit range of intensities (flash intensities $\sim 10^{12}$ - $10^{14.5}$ photons/cm²/s; note that a different set of spectral stimuli were used with dLGN and ERG experiments, owing to technical constraints). Light flashes were superimposed on a short or long wavelength background light (450 and 550nm respectively, bandwidth ± 40 nm), designed to suppress rod activity ($\sim 10^{13.5}$ effective photons/cm²/s), and bias responses in favour of cones. The backgrounds also represented an opportunity to confirm the UV peak of SWS opsin sensitivity. Thus, while both backgrounds had equivalent effective intensity for MWS-cones (respectively $10^{13.4}$ and $10^{13.6}$ effective photons/cm²/s), even the shorter wavelength should have negligible impact on SWS-cones with a λ_{\max} of 360nm ($10^{10.5}$ effective photons/cm²/s). In this way, we expect both wavelengths to suppress MWS more than SWS-cone responses. Conversely, if the *Rhabdomys* SWS opsin had $\lambda_{\max} > 400$ nm we expect marked suppression of short wavelength responses in the presence of our short (but not long) wavelength background light.

With this approach, we were able to describe the spectral sensitivity of light-evoked responses from 189 single neurons. Two distinct patterns of spectral sensitivity emerged: one group of neurons (n=42) exhibited strong responses to only the shortest wavelength (425nm) flashes (Fig 7a,c), consistent with an SWS-cone dependent origin. The other group of neurons (n=147) responded to all wavelengths with a sensitivity consistent with a strong MWS-cone bias (Fig 7b,d). Since, for both groups of neurons, responses were essentially identical under short and long-wavelength backgrounds (Fig 7a-d), subsequent analyses used the average response across both backgrounds. Corresponding single opsin spectral sensitivity estimates for individual cells (Fig 7e) were strongly clustered around ~500nm (mean \pm SEM= 501 \pm 3nm for the 5 best fitting cells; >95% variance explained) or <400nm (tested wavelengths did not provide reliable discrimination at shorter wavelengths but results are fully compatible with a λ_{\max} =360nm). Consistent then with the ERG data described above, across the entire population of LGN neurons, overall spectral sensitivity could be very well explained by a combination of two pigments with λ_{\max} of 360 and 501nm (Fig 7f,g). In this case however, effective SWS-cone contributions were much stronger than observed in ERG studies (Fig 7g, best fit ratio of 65:1; $r^2=0.99$). This can be explained by the presence of the adapting background lights, which are predicted to suppress sensitivity of pigments with $\lambda_{\max} > 400$ nm (in this case MWS but not UVS cone opsins). This observation (and the similarity in responses under the two tested backgrounds) thus represents further support for the hypothesis of a UV peak sensitivity for *Rhabdomys* SWS opsin.

We also applied this protocol under scotopic conditions following 30 minutes dark adaptation, and using stimuli 4 log units dimmer than in light adapted conditions (flash intensities $\sim 10^8$ - $10^{10.5}$ photons/cm²/s). In these conditions, we would expect rod photoreception to dictate the sensitivity of the resulting responses. Across 31 neurons that exhibited robust responses under these conditions (Fig 8a), we determined which single opsin could best account for the observed pattern of responses, using an approach equivalent to that described above (Fig 8b). As expected from the rod spectral sensitivity of other mammals, the estimates of λ_{\max} were tightly clustered at values just below 500nm (Fig 8c). Among these cells, the group whose responses could be best explained by the spectral sensitivity of a single opsin (>80% variance in responses accounted for) had λ_{\max} =493 \pm 3nm (mean \pm SEM, n=7; Fig 8c-e).

Estimating the impact of the *Rhabdomys* lens on SWS and MWS opsins.

Our data all support the notion that the lens of *Rhabdomys* has a low transmission for wavelengths <400 nm, but an SWS opsin with λ_{\max} approximately 360 nm. To provide some real-world context to these values, we assessed the expected excitation of *Rhabdomys* and mouse SWS and MWS opsins in daylight. Using environmentally measured spectrum of sunlight, we asked how the predicted excitation of SWS and MWS opsins was impacted by lens transmission in *Rhabdomys* and mice (figure 2). We observed a reduction of approximately 70% in the excitation of the *Rhabdomys* SWS opsin, compared with ~15% in the mouse (for MWS opsins in each species, the impact of lens transmission is minimal). Note however, that despite the increased impact of the *Rhabdomys* lens on the SWS opsin, its relative excitation in daylight remains well above threshold (and within the range of Weber adaptation), suggesting reasonable UV sensitivity despite low transmission of the *Rhabdomys* lens for wavelengths <400nm.

Discussion

We set out to examine the *in vivo* spectral sensitivity of the visual system of the diurnal rodent, *Rhabdomys pumilio*, and establish the extent to which its visual system is consistent with its diurnal lifestyle. The *Rhabdomys* retina contains two classes of cones, rods, and ipRGCs. As with other diurnal species, the *Rhabdomys* eye contains a cone-rich retina. Both amino acid sequence analysis and electrophysiological recordings are consistent with the conclusion that the spectral sensitivity of SWS and MWS-cones is similar to that of closely related nocturnal species. However, the presence of a long-pass lens appears to greatly impacts sensitivity to shorter wavelengths, producing anomalous narrow-band spectral tuning of *Rhabdomys* SWS-cones.

Our functional data are consistent with the previous reports that the *Rhabdomys* retina is cone dominated, (>50% cone photoreceptors (van der Merwe et al. 2018)). We reveal robust cone-evoked ERG responses that can track stimuli inverting at high temporal frequencies ($\leq 40\text{Hz}$), and robust, large amplitude responses across the high light levels tested here. Similarly, LGN responses are more numerous and robust under cone-favouring photopic conditions. Previous immunohistochemical analyses have established that the *Rhabdomys* retina contains two cone opsins (SWS and MWS (van der Merwe et al. 2018)), with higher expression of MWS opsin (as often observed in such rodent species). We were able to clone and sequence both *Rhabdomys* cone opsins, and a comparison with related rodent species (both nocturnal and diurnal) revealed very close sequence homology with mouse and rat SWS/MWS opsins, predicting similarities in their spectral sensitivity. In agreement with this prediction both ERG and dLGN recordings revealed that, while sensitivity across the human visible spectrum was consistent with that of a single photopigment with λ_{\max} around 500nm, responses to near UV wavelengths were anomalously sensitive. One obvious potential origin for high UV sensitivity is intra-ocular fluorescence. However, this does not provide an adequate explanation for our data, as we find that a subset of dLGN neurons respond only to 425nm, not the longer wavelengths that should be the product of fluorescence. Moreover, a background light that should suppress responses from any SWS pigment with peak sensitivity in the human visible range did not impact responses to the shorter wavelengths. These findings argue that there is indeed a photoreceptor specifically sensitive to very short wavelength light and that the *Rhabdomys* SWS pigment has $\lambda_{\max} \sim 400\text{nm}$.

Direct electrophysiological or microspectrophotometrical assessments of cone photoreceptors *ex vivo*, or absorbance spectroscopy of purified cone pigments *in vitro*, would be a valuable complement to the current dataset in refining our estimate for cone opsin spectral sensitivity. In particular, while our data clearly show that SWS-opsin sensitivity peaks in the near UV, the UV light filtering properties of the *Rhabdomys* lens make it challenging to precisely define its λ_{\max} based upon *in vivo* physiological responses. Unfortunately, our attempts to overcome this by recording retinal ganglion cell activity *ex vivo* using a multielectrode array were hindered by *Rhabdomys*' thick inner limiting membrane. Our best estimate is that the SWS-opsin λ_{\max} lies around 360nm. First, the ERG revealed photopic spectral sensitivity that was best

described by the weighted sum of two nomograms, with λ_{\max} of 360nm and ~500nm, and ratio of ~1:4. Secondly, we assessed the spectral sensitivity in the visual thalamus of anaesthetised *Rhabdomys*. Here, responses of individual neurons could be well described by single opsin spectral sensitivity estimates. Approximately 75% of neurons with λ_{\max} ~500nm, and the remaining neurons with λ_{\max} <400nm (tested wavelengths did not provide reliable discrimination at shorter wavelengths but results are fully compatible with a λ_{\max} =360nm). Likewise, across the population of dLGN neurons we recorded, overall spectral sensitivity could be very well explained by a combination of two pigments with λ_{\max} of 360 and 501nm. Lastly, we were able to validate these putative λ_{\max} values by applying the technique of receptor silent substitution. In this case, a pair of spectrally distinct stimuli, designed to be isoluminant for pigments with λ_{\max} of 360nm and 500nm, evoked no measurable ERG response.

We also explored the spectral sensitivity of *Rhabdomys* vision in the dLGN under conditions of dark adaptation. These data indicated a λ_{\max} of ~493nm, which is typical for rod vision in terrestrial mammals (classically ~500nm). However, light adaptation and/or a change in temporal frequency to bias responses towards cones produced only a small shift in spectral sensitivity, with MWS-cones having a λ_{\max} shifted approximately 7nm towards longer wavelength. This similarity indicates that there is a limited adjustment in the spectral sensitivity of *Rhabdomys* vision across the day-night cycle – or a low-amplitude Purkinje shift.

While the presumed spectral sensitivity of *Rhabdomys* cone (and rod) opsins are remarkably similar to those of its close nocturnal relatives, the filtering properties of the *Rhabdomys* lens attenuates the amount of short-wavelength light actually reaching the *Rhabdomys* retina. To put this into some context, the *Rhabdomys* lens attenuates the activation of the SWS-cone to natural daylight by ~70% (compared with the mouse lens which is close to ~ 15%). While a long-pass property is a common feature of lenses in diurnal animals, it is most commonly paired with a concurrent shift in opsin spectral sensitivity towards longer wavelengths. To our knowledge, a combination of <400nm SWS opsin λ_{\max} and UV-filtering lens is highly unusual throughout the animal kingdom (Ellingson et al. 1995). This pairing, in effect, means that SWS-cone sensitivity is dramatically curtailed at shorter wavelengths to leave it responsive to only a narrow portion of the spectrum. But despite this narrowing in sensitivity, we find evidence that the *Rhabdomys* SWS-cone contributes to activity throughout the visual projection. The utility of this more narrow-band UV sensitive pigment in *Rhabdomys*, however, remains a matter of speculation. The most parsimonious explanation is that this combination is a compromise, on the one hand restricting the amount of UV light reaching the *Rhabdomys* retina (to protect the retina from damage and/or enhance acuity); and on the other, retaining enough 'functional' UV sensitivity for a particular purpose. One possible reason for this UV sensitivity could be to allow violet-green colour discrimination (e.g. (Joesch and Meister 2016)). The presence of separate cone classes expressing SWS and MWS opsins supports the notion. We have not explicitly tested that hypothesis in the current study; though it is notable that SWS and MWS evoked responses appear to remain separate at least at the level of the visual thalamus, implying that chromatic discrimination would be available to higher level visual processing. An alternative function could relate to evidence that shorter-wavelength sensitivity can enhance contrast detection for light coming from the sky (Baden et al. 2013), which could improve detection of overhead predators.

Our findings have implications for using *Rhabdomys* as a laboratory organism. Diurnal rodents could be useful alternatives to non-human primates and companion-animal species for examining cone/photopic vision. *Rhabdomys* can be maintained as a breeding colony in standard rodent facilities (provided that they receive appropriate environmental enrichment) and are reliably diurnal in both the laboratory and wild. This first description of their visual physiology confirms the presence of adaptations to a diurnal niche in their visual system and their potential for studying cone-based vision.

Acknowledgements

We would like to thank the Hoekstra lab at Harvard University for the original *Rhabdomys* breeding pairs used to establish our colony, and members of the BSF at the University of Manchester for assistance in husbandry and colony maintenance. We would also like to thank Jonathan Wynne, Dr Krys Procyk and Dr Nina Milosavljevic for their assistance with immunohistochemistry. This work was supported by grants from the BBSRC (BB/P009182/1) and the Wellcome Trust (210684/Z/18/Z) to RJL, and the BBSRC (B/N014901/1) to TMB and RJL. AEA was supported by a University of Manchester Dean's prize Fellowship.

Figure Captions

Figure 1. Alignment of *Rhabdomys* SWS and MWS opsins, aligned with sequences of rodent species. **a)** *Rhabdomys* (Rhabdo) SWS opsin against the following species: *Mus musculus* (mouse, NP_031564.1), *Rattus norvegicus* (rat, NP_112277.1), *Meriones unguiculatus* (gerbil; XP_021517546.1), *Octodon degus* (degu; XP_004642783.1), *Ictidomys tridecemlineatus* (thirteen-lined ground squirrel (TLG); XP_021578083.1) and *Cavia porcellus* (guinea pig; NP_001166229). *Rhabdomys* SWS opsin structure is based on mouse SWS1 opsin structure and is shown by labelled coloured bars where: TM = transmembrane domain, IC = intracellular loops, and EC = extracellular loops. Key sites are shown in bold and underlined: UV tuning site 86, counterion site 113, and retinal binding site 296. **b)** Alignment of *Rhabdomys* MWS opsin against the following species: *Mus musculus* (NP_032132.1), *Rattus norvegicus* (NP_446000.1), *Meriones unguiculatus* (XP_021484930.1), *Octodon degus* (XP_023561139.1), *Cavia porcellus* (NP_001166460.1) and *Ictidomys tridecemlineatus* (AAW29517.1). *Rhabdomys* MWS opsin structure is based on mouse MWS opsin structure and is shown by labelled coloured bars as in **a**. Key sites are shown in bold and underlined: counterion site 113, retinal binding site 296 and LWS/MWS spectral tuning sites: 164, 181, 261, 269 and 292. Numbering of key sites based on bovine rod opsin. All alignments performed using MAFFT (Kato and Standley 2013).

Figure 2. Anatomical features of *Rhabdomys* retina and transmission of *Rhabdomys* lens. **a)** Immunohistochemistry for MWS (cyan) and SWS (pink) opsins on retinal wholemount. Left panel: overlay; middle panel: MWS opsin; right panel: SWS opsin. Scale bars: 25 μ m **b)** Sagittal section of *Rhabdomys* eye following cresyl violet staining, showing lens (**L**) and neural retina (**R**). **c)** Spectral transmission of 5 *Rhabdomys* lenses (black lines) and group mean (purple line), and the group mean of 16 mouse lenses (green line), from 300-700nm. All values are normalised to transmission at 700nm.

Figure 3. Spectral sensitivity of ERG responses in response to a dark-adapted flash. **a)** Representative ERG responses to flicker stimuli of different frequencies. **b)** Response amplitude of flicker stimuli of different frequencies ($n = 3$; data shows mean \pm SEM). **c)** Spectral power distribution of 13 stimuli used to track spectral sensitivity. **d)** Representative flash ERGs for spectral stimuli presented at maximum intensity. **e)** Normalised b-wave amplitude for spectral stimuli presented at up to 6 intensities ($n = 3$; data shows mean \pm SEM). **f)** Mean \pm SEM EC50 values plotted as a function of wavelength (central peak of each channel). Black line shows best fitting spectral sensitivity function (accounting for lens transmission) to describe these data ($\lambda_{max} = 501$; R^2 of 0.978). Note that 635 and 660nm data points are excluded given the low sensitivity to these wavelengths. **g)** Response amplitude as a function of effective photon flux for best fitting nomogram/pair of nomograms. In this case, the best fit was comprised of two pigments with λ_{max} of 360 and 504, at a ratio of 1:6. The curve fit has an R^2 of 0.999 **h)** Spectral sensitivity function of best fitting nomogram/pair of nomograms (used to generate x axis in g). EC50 values replotted from **f** for comparison.

Figure 4. Spectral sensitivity of ERG responses in response to a 32Hz flicker. **a)** Representative ERG responses to maximum intensity spectral stimuli presented as a 32Hz flicker **b)** Normalised response amplitude for spectral stimuli presented at up to 6 intensities ($n = 3$; data shows mean \pm SEM). Note that 635 and 660nm data points are excluded given the low sensitivity to these wavelengths. **c)** Mean \pm SEM EC50 values plotted as a function of

wavelength (central peak of each channel). Black line shows best fitting spectral sensitivity function (accounting for lens transmission) to describe these data ($\lambda_{\max} = 503$; R^2 of 0.969). **d**) Response amplitude as a function of effective photon flux for best fitting nomogram/pair of nomograms. In this case, the best fit was comprised of two pigments with λ_{\max} of 360 and 500, at a ratio of 1:4. The curve fit has an R^2 of 0.996 ($n = 3$). **e**) Spectral sensitivity function of best fitting nomogram/pair of nomograms (used to generate x axis in D). EC50 values replotted from **c** for comparison.

Figure 5. Spectral sensitivity of ERG responses in light-adapted conditions. **a**) Spectral power distribution of background light. **b**) Normalised response amplitude for 32Hz flicker, measured across 3 intensities for each spectral stimulus, and in the presence of an adapting background light ($n = 3$; data shows mean \pm SEM). **c**) In the presence of background light, data were best fit with a pair of nomograms with λ_{\max} of 360 and 503, at a ratio of 1:10 ($R^2=0.992$; $n = 3$).

Figure 6. Silent substitution ERG responses **a**) Pair of spectra (termed 'Stimulus' and 'Background') designed to be isoluminant for putative *Rhabdomys* SWS and MWS cone opsins (accounting for lens transmission). **b**) ERG response of two *Rhabdomys* to a transition between the spectral pair (10ms flash of 'Stimulus' spectrum, interleaved with 990ms of 'Background' spectrum). **c**) Pair of spectra designed to be isoluminant for putative *Rhabdomys* MWS cone opsin, but presenting 99% contrast for putative *Rhabdomys* SWS cone opsin (accounting for lens transmission). **d**) ERG response of two *Rhabdomys* to a transition between this spectral pair (10ms flash of 'Stimulus' spectrum, interleaved with 990ms of 'Background' spectrum).

Figure 7. Spectral sensitivity of LGN neuron responses under light-adaptation. **a,b**) representative responses of two *Rhabdomys* LGN neurons 1s moderate and bright light flashes (means of 20 trials) of varying wavelength under short and long-wavelength adaptation (450 and 550nm respectively, bandwidth ± 40 nm; $10^{13.5}$ rod-effective photons/cm²/s). **c,d**) Irradiance response relationships for neurons in **a** and **b** with irradiance quantified according to the effective (lens-corrected) photon flux for a single opsin with a λ_{\max} of 360nm (**c**) and 501nm. Note differing range of x axes. **d**). Insets show spectral sensitivity estimates under short and long wavelength adaptation; note that tested wavelengths offered little discriminatory power for $\lambda_{\max} < 400$ nm). **e**) Population spectral sensitivity estimates ($n=189$ neurons, based on average responses across short and long wavelength backgrounds) showing best-fitting single opsin λ_{\max} and corresponding response variance explained. **f**) Normalised mean \pm SEM irradiance response relationships for all LGN cells that responded under light adapted conditions, fit with 4-parameter sigmoid curves. **g**) Sensitivity estimates (from **f**), best-fit to a pair of *Rhabdomys* lens corrected opsin templates with $\lambda_{\max} = 360$ and 501nm at a ratio of 65:1($r^2=0.99$).

Figure 8. Spectral sensitivity of LGN neuron responses under scotopic conditions. **a**) Representative responses of a *Rhabdomys* LGN neuron to 1s dim light flashes (means of 20 trials) of varying intensity and wavelength under dark adapted conditions. **b**) Irradiance response relationship for neuron in **a** with irradiance quantified according to the effective photon flux for a single opsin with a λ_{\max} of 493nm (corrected for *Rhabdomys* lens transmission). Inset shows spectral sensitivity estimate (quantified as the %variance in effective irradiance response curves explained by the best fitting 4-parameter sigmoid curve). **c**) Population spectral sensitivity estimates showing best-fitting single opsin λ_{\max} and corresponding response variance explained (as in **b**). **d**) Normalised mean \pm SEM irradiance response relationships for cells whose responses were best explained by a single opsin (>80% variance explained, highlighted in red in **c**), fit with 4-parameter sigmoid curves. **e**) Sensitivity estimates (from **d**), fit to a *Rhabdomys* lens corrected opsin template with $\lambda_{\max} = 493$ nm ($r^2=0.99$).

Table 1

	<i>Mus musculus</i>	<i>Rattus norvegicus</i>	<i>Octodon degus</i>	<i>Meriones unguiculatus</i>	<i>Ictidomys tridecemlineatus</i>	<i>Cavia porcellus</i>
SWS	96%	96%	93%	91%	90%	88%
MWS	97%	97%	x	93%	93%	89%

Table 1 – Sequence homology of *Rhabdomys* SWS and MWS opsins following alignment with a selection of nocturnal and diurnal rodents. Table shows % homology between *Rhabdomys* and other rodent SWS/MWS opsins. Note no comparison with *Octodon degus* MWS opsin due to missing sequence data for N-terminus.

Table 2

	SWS effective photons/cm ² /s		MWS effective photons/cm ² /s	
	Without lens	With lens	Without lens	With lens
<i>Rhabdomys</i>	6.44 x10 ¹⁴	1.93 x10 ¹⁴	4.73 x10 ¹⁴	4.36 x10 ¹⁴
Mouse	7.35 x10 ¹⁴	4.9 x10 ¹⁴	4.98 x10 ¹⁴	4.49 x10 ¹⁴

Table 2 – Impact of *Rhabdomys* and mouse lens transmission on the excitation of SWS and MWS pigments. Table shows predicted effective photon flux for *Rhabdomys* and mouse SWS and MWS opsins, with and without lens transmission, in natural daylight.

References

- Ahnelt, P. K. and H. Kolb** (2000). The mammalian photoreceptor mosaic-adaptive design. *Progress in Retinal and Eye Research* **19**(6): 711-777.
- Allen, A. E. and R. J. Lucas** (2016). Using Silent Substitution to Track the Mesopic Transition From Rod- to Cone-Based Vision in Mice. *Invest Ophthalmol Vis Sci* **57**(1): 276-287.
- Allen, A. E., R. Storchi, F. P. Martial, R. S. Petersen, M. A. Montemurro, T. M. Brown and R. J. Lucas** (2014). Melanopsin-driven light adaptation in mouse vision. *Curr Biol* **24**(21): 2481-2490.
- Applebury, M. L., M. P. Antoch, L. C. Baxter, L. L. Chun, J. D. Falk, F. Farhangfar, K. Kage, M. G. Krzystolik, L. A. Lyass and J. T. Robbins** (2000). The murine cone photoreceptor: a single cone type expresses both S and M opsins with retinal spatial patterning. *Neuron* **27**(3): 513-523.
- Baden, T., T. Schubert, L. Chang, T. Wei, M. Zaichuk, B. Wissinger and T. Euler** (2013). A tale of two retinal domains: near-optimal sampling of achromatic contrasts in natural scenes through asymmetric photoreceptor distribution. *Neuron* **80**(5): 1206-1217.
- Blanga-Kanfi, S., H. Miranda, O. Penn, T. Pupko, R. W. DeBry and D. Huchon** (2009). Rodent phylogeny revised: analysis of six nuclear genes from all major rodent clades. *BMC Evol Biol* **9**: 71.
- Brown, T. M., S. Tsujimura, A. E. Allen, J. Wynne, R. Bedford, G. Vickery, A. Vugler and R. J. Lucas** (2012). Melanopsin-based brightness discrimination in mice and humans. *Curr Biol* **22**(12): 1134-1141.
- Cameron, M. A. and R. J. Lucas** (2009). Influence of the rod photoresponse on light adaptation and circadian rhythmicity in the cone ERG. *Mol Vis* **15**: 2209-2216.

- Cowing, J. A., S. Poopalasundaram, S. E. Wilkie, P. R. Robinson, J. K. Bowmaker and D. M. Hunt** (2002). The molecular mechanism for the spectral shifts between vertebrate ultraviolet- and violet-sensitive cone visual pigments. *Biochem J* **367**(Pt 1): 129-135.
- Dewsbury, D. A. and W. W. Dawson** (1979). African 4-Striped Grass Mice (*Rhabdomys Pumilio*), a Diurnal-Crepuscular Muroid Rodent, in the Behavioral Laboratory. *Behav Res Meth Instr* **11**(3): 329-333.
- Douglas, R. H. and G. Jeffery** (2014). The spectral transmission of ocular media suggests ultraviolet sensitivity is widespread among mammals. *P Roy Soc B-Biol Sci* **281**(1780): 20132995.
- Douglas, R. H. and G. Jeffery** (2014). The spectral transmission of ocular media suggests ultraviolet sensitivity is widespread among mammals. *Proc Biol Sci* **281**(1780): 20132995.
- Ellingson, J. M., L. J. Fleishman and E. R. Loew** (1995). Visual pigments and spectral sensitivity of the diurnal gecko *Gonatodes albogularis*. *J Comp Physiol A* **177**(5): 559-567.
- Emerling, C. A., H. T. Huynh, M. A. Nguyen, R. W. Meredith and M. S. Springer** (2015). Spectral shifts of mammalian ultraviolet-sensitive pigments (short wavelength-sensitive opsin 1) are associated with eye length and photic niche evolution. *Proc Biol Sci* **282**(1819).
- Fasick, J. I., M. L. Applebury and D. D. Oprian** (2002). Spectral tuning in the mammalian short-wavelength sensitive cone pigments. *Biochemistry* **41**(21): 6860-6865.
- Gibson, D. G., L. Young, R. Y. Chuang, J. C. Venter, C. A. Hutchison, 3rd and H. O. Smith** (2009). Enzymatic assembly of DNA molecules up to several hundred kilobases. *Nat Methods* **6**(5): 343-345.
- Govardovskii, V. I., N. Fyhrquist, T. Reuter, D. G. Kuzmin and K. Donner** (2000). In search of the visual pigment template. *Vis Neurosci* **17**(4): 509-528.
- Hunt, D. M., L. S. Carvalho, J. A. Cowing and W. L. Davies** (2009). Evolution and spectral tuning of visual pigments in birds and mammals. *Philos Trans R Soc Lond B Biol Sci* **364**(1531): 2941-2955.
- Hunt, D. M., L. S. Carvalho, J. A. Cowing, J. W. Parry, S. E. Wilkie, W. L. Davies and J. K. Bowmaker** (2007). Spectral tuning of shortwave-sensitive visual pigments in vertebrates. *Photochem Photobiol* **83**(2): 303-310.
- Hunt, D. M., J. A. Cowing, S. E. Wilkie, J. W. Parry, S. Poopalasundaram and J. K. Bowmaker** (2004). Divergent mechanisms for the tuning of shortwave sensitive visual pigments in vertebrates. *Photochem Photobiol Sci* **3**(8): 713-720.
- Hut, R. A., N. Kronfeld-Schor, V. van der Vinne and H. De la Iglesia** (2012). In search of a temporal niche: environmental factors. *Prog Brain Res* **199**: 281-304.
- Jacobs, G. H.** (1993). The distribution and nature of colour vision among the mammals. *Biol Rev Camb Philos Soc* **68**(3): 413-471.
- Joesch, M. and M. Meister** (2016). A neuronal circuit for colour vision based on rod-cone opponency. *Nature* **532**(7598): 236-239.
- Katoh, K. and D. M. Standley** (2013). MAFFT multiple sequence alignment software version 7: improvements in performance and usability. *Mol Biol Evol* **30**(4): 772-780.
- Krishna, V. R., K. R. Alexander and N. S. Peachey** (2002). Temporal properties of the mouse cone electroretinogram. *J Neurophysiol* **87**(1): 42-48.
- Kryger, Z., L. Galli-Resta, G. H. Jacobs and B. E. Reese** (1998). The topography of rod and cone photoreceptors in the retina of the ground squirrel. *Vis Neurosci* **15**(4): 685-691.
- Lind, O., M. Mitkus, P. Olsson and A. Kelber** (2014). Ultraviolet vision in birds: the importance of transparent eye media. *P Roy Soc B-Biol Sci* **281**(1774).
- Pachitariu, M., N. Steinmetz, S. Kadir, M. Carandini and K. D. Harris** (2016). Kilosort: realtime spike-sorting for extracellular electrophysiology with hundreds of channels. *BioRxiv*.
- Peichl, L.** (2005). Diversity of mammalian photoreceptor properties: adaptations to habitat and lifestyle? *Anat Rec A Discov Mol Cell Evol Biol* **287**(1): 1001-1012.
- Qian, H., M. R. Shah, K. R. Alexander and H. Ripps** (2008). Two distinct processes are evident in rat cone flicker ERG responses at low and high temporal frequencies. *Exp Eye Res* **87**(1): 71-75.

- Sagdullaev, B. T., P. J. DeMarco and M. A. McCall** (2004). Improved contact lens electrode for corneal ERG recordings in mice. *Doc Ophthalmol* **108**(3): 181-184.
- Schumann, D. M., H. M. Cooper, M. D. Hofmeyr and N. C. Bennett** (2005). Circadian rhythm of locomotor activity in the four-striped field mouse, *Rhabdomys pumilio*: A diurnal African rodent. *Physiol Behav* **85**(3): 231-239.
- Schumann, D. M., H. M. Cooper, M. D. Hofmeyr and N. C. Bennett** (2006). Light-induced Fos expression in the suprachiasmatic nucleus of the four-striped field mouse, *Rhabdomys pumilio*: A southern African diurnal rodent. *Brain Res Bull* **70**(4-6): 270-277.
- van der Merwe, I., A. Lukats, V. Blahova, M. K. Oosthuizen, N. C. Bennett and P. Nemeč** (2018). The topography of rods, cones and intrinsically photosensitive retinal ganglion cells in the retinas of a nocturnal (*Micaelamys namaquensis*) and a diurnal (*Rhabdomys pumilio*) rodent. *PLoS One* **13**(8): e0202106.
- van Norren, D. and T. G. M. F. Gorgels** (2011). The Action Spectrum of Photochemical Damage to the Retina: A Review of Monochromatic Threshold Data. *Photochem Photobiol* **87**(4): 747-753.
- Yokoyama, S. and F. B. Radlwimmer** (1998). The "five-sites" rule and the evolution of red and green color vision in mammals. *Mol Biol Evol* **15**(5): 560-567.

A

N-terminus **TM1**

Rhabdo ---MSGEDDFYLFKNISSVGGPDGQYHIAVWAFHLQAAMFGVFFVGTPLNAIVLVAT 57
 Mouse ---MSGEDDFYLFQNISSVGGPDGQYHIAVWAFHLQAAMFGVFFVGTPLNAIVLVAT
 Rat ---MSGEXEYFLFQNISSVGGPDGQYHIAVWAFHLQAAMFGVFFVGTPLNAIVLVAT
 Gerbil ---MSGEDDFYLFQNISSVGGPDGQYHIAVWAFHLQAAMFGVFFVGTPLNAIVLVAT
 Degu ---MSKEEYFLFQNISSVGGPDGQYHIAVWAFHLQAAMFGVFFVGTPLNAIVLVAT
 Guinea ---MSKEEYFLFQNISSVGGPDGQYHIAVWAFHLQAAMFGVFFVGTPLNAIVLVAT
 TLG MNTMSEEEFFLFRNISSVGGPDGQYHIAVWAFHLQAAMFGVFFVGTPLNAIVLVAT

IC1 **TM2** **EC1** **TM3**

Rhabdo LHYKKLRQPLNYILVNVSLGGFLICIFSVFTVFIASCHGYFLFGRHVCALEAFGLGSVAGL 117
 Mouse LHYKKLRQPLNYILVNVSLGGFLICIFSVFTVFIASCHGYFLFGRHVCALEAFGLGSVAGL
 Rat LHYKKLRQPLNYILVNVSLGGFLICIFSVFTVFIASCHGYFLFGRHVCALEAFGLGSVAGL
 Gerbil LHYKKLRQPLNYILVNVSLGGFLICIFSVFTVFIASCHGYFLFGRHVCALEAFGLGSVAGL
 Degu LHYKKLRQPLNYILVNVSLGGFLICIFSVFTVFIASCHGYFLFGRHVCALEAFGLGSVAGL
 Guinea LHYKKLRQPLNYILVNVSLGGFLICIFSVFTVFIASCHGYFLFGRHVCALEAFGLGSVAGL
 TLG LRYKKLRQPLNYILVNVSLGGFLICIFSVFTVFIASCHGYFLFGRHVCALEAFGLGSVAGL

UV tuning site **Counterion**

IC2 **TM4**

Rhabdo VTGWSLAFALAFERYIVICKPFGNFRFSSKHALVVLVLTWIIIGIGVSIPIFFGWSRFIPEG 177
 Mouse VTGWSLAFALAFERYIVICKPFGNFRFSSKHALVVLVLTWIIIGIGVSIPIFFGWSRFIPEG
 Rat VTGWSLAFALAFERYIVICKPFGNFRFSSKHALVVLVLTWIIIGIGVSIPIFFGWSRFIPEG
 Gerbil VTGWSLAFALAFERYIVICKPFGNFRFSSKHALVVLVLTWIIIGIGVSIPIFFGWSRFIPEG
 Degu VTGWSLAFALAFERYIVICKPFGNFRFSSKHALVVLVLTWIIIGIGVSIPIFFGWSRFIPEG
 Guinea VTGWSLAFALAFERYIVICKPFGNFRFSSKHALVVLVLTWIIIGIGVSIPIFFGWSRFIPEG
 TLG VTGWSLAFALAFERYIVICKPFGNFRFSSKHALVVLVLTWIIIGIGVSIPIFFGWSRFIPEG

EC2 **TM5** **IC3**

Rhabdo LQCSGPDWYVGTGKYRSEYITWFLIFCFIIPLSLILCFYSQGLRLTRAVAAQQQESAT 237
 Mouse LQCSGPDWYVGTGKYRSEYITWFLIFCFIIPLSLILCFYSQGLRLTRAVAAQQQESAT
 Rat LQCSGPDWYVGTGKYRSEYITWFLIFCFIIPLSLILCFYSQGLRLTRAVAAQQQESAT
 Gerbil LQCSGPDWYVGTGKYRSEYITWFLIFCFIIPLSLILCFYSQGLRLTRAVAAQQQESAT
 Degu LQCSGPDWYVGTGKYRSEYITWFLIFCFIIPLSLILCFYSQGLRLTRAVAAQQQESAT
 Guinea LQCSGPDWYVGTGKYRSEYITWFLIFCFIIPLSLILCFYSQGLRLTRAVAAQQQESAT
 TLG LQCSGPDWYVGTGKYRSEYITWFLIFCFIIPLSLILCFYSQGLRLTRAVAAQQQESAT

TM6 **EC3** **TM7**

Rhabdo TQKAEREVSHMVMVMSGFCVYVYAAALAMYVNNRNHGLDLRLVTVPAFFSKSSCVYN 297
 Mouse TQKAEREVSHMVMVMSGFCVYVYAAALAMYVNNRNHGLDLRLVTVPAFFSKSSCVYN
 Rat TQKAEREVSHMVMVMSGFCVYVYAAALAMYVNNRNHGLDLRLVTVPAFFSKSSCVYN
 Gerbil TQKAEREVSHMVMVMSGFCVYVYAAALAMYVNNRNHGLDLRLVTVPAFFSKSSCVYN
 Degu TQKAEREVSHMVMVMSGFCVYVYAAALAMYVNNRNHGLDLRLVTVPAFFSKSSCVYN
 Guinea TQKAEREVSHMVMVMSGFCVYVYAAALAMYVNNRNHGLDLRLVTVPAFFSKSSCVYN
 TLG TQKAEREVSHMVMVMSGFCVYVYAAALAMYVNNRNHGLDLRLVTVPAFFSKSSCVYN

C-terminus

Rhabdo PIIYCFMKNQFRACILEMVCRCRPMADSDMSGSKTEVSTVSSKVGPH 346
 Mouse PIIYCFMKNQFRACILEMVCRCRPMADSDMSGSKTEVSTVSSKVGPH
 Rat PIIYCFMKNQFRACILEMVCRCRPMADSDMSGSKTEVSTVSSKVGPH
 Gerbil PIIYCFMKNQFRACILEMVCRCRPMADSDMSGSKTEVSTVSSKVGPH
 Degu PIIYCFMKNQFRACILEMVCRCRPMADSDMSGSKTEVSTVSSKVGPH
 Guinea PIIYCFMKNQFRACILEMVCRCRPMADSDMSGSKTEVSTVSSKVGPH
 TLG PIIYCFMKNQFRACILEMVCRCRPMADSDMSGSKTEVSTVSSKVGPH

B

N-terminus

Rhabdo MAQR----LTGEQTSDDHYEDSTHSSIFTYTNSNSTKRGPFEGPNYHIAPRVYVHLTSTAM 55
 Mouse MAQR----LTGEQTLDDHYEDSTHSSIFTYTNSNSTKRGPFEGPNYHIAPRVYVHLTSTAM
 Rat MAQQ----LTGEQTLDDHYEDSTHSSIFTYTNSNSTKRGPFEGPNYHIAPRVYVHLTSTAM
 Gerbil MAQR----LTGEQTLDDHYEDSTHSSIFTYTNSNSTKRGPFEGPNYHIAPRVYVHLTSTAM
 Degu MAQR----LTGEQTLDDHYEDSTHSSIFTYTNSNSTKRGPFEGPNYHIAPRVYVHLTSTAM
 Guinea MAQRWGFPHALSGVQAQDAEDYSTQASLFTYTNNSNTRGPFEGPNYHIAPRVYVHLTSTAM

TM1 **IC1** **TM2**

Rhabdo ILVVVASVFTNGLVLAATMRFKLRHPLMILVNLAVADLAETIIASTISVNVQIYGYFV 115
 Mouse ILVVVASVFTNGLVLAATMRFKLRHPLMILVNLAVADLAETIIASTISVNVQIYGYFV
 Rat ILVVVASVFTNGLVLAATMRFKLRHPLMILVNLAVADLAETIIASTISVNVQIYGYFV
 Gerbil IFVVVIASVFTNGLVLAATMRFKLRHPLMILVNLAVADLAETIIASTISVNVQIYGYFV
 Degu VIIVVIASVFTNGLVLAATMRFKLRHPLMILVNLAVADLAETIIASTISVNVQIYGYFV
 Guinea TIVVIASIFTNGLVLAATMRFKLRHPLMILVNLAVADLAETIIASTISVNVQIYGYFV

EC1 **TM3** **IC2** **TM4**

Rhabdo LGHPLCVIEGYIVSLCGITGLWSLAIISWERLWLVCKPFGNVRFDKALATVGIIVFSVWVA 175
 Mouse LGHPLCVIEGYIVSLCGITGLWSLAIISWERLWLVCKPFGNVRFDKALATVGIIVFSVWVA
 Rat LGHPLCVIEGYIVSLCGITGLWSLAIISWERLWLVCKPFGNVRFDKALATVGIIVFSVWVA
 Gerbil LGHPLCVIEGYIVSLCGITGLWSLAIISWERLWLVCKPFGNVRFDKALATVGIIVFSVWVA
 Degu LGYPLCVIEGYIVSLCGITGLWSLAIISWERLWLVCKPFGNVRFDKALATVGIIVFSVWVA
 Guinea LGHPLCVIEGYIVSLCGITGLWSLAIISWERLWLVCKPFGNVRFDKALATVGIIVFSVWVA

Counterion **Site 164**

TM4 **EC2** **TM5**

Rhabdo AVWTAPPVIFGWSRYWYFGLKTSVCGDFVSGTSPGVQSYMMVLMVTCIIFPLSIIIVLCYL 235
 Mouse AVWTAPPVIFGWSRYWYFGLKTSVCGDFVSGTSPGVQSYMMVLMVTCIIFPLSIIIVLCYL
 Rat AVWTAPPVIFGWSRYWYFGLKTSVCGDFVSGTSPGVQSYMMVLMVTCIIFPLSIIIVLCYL
 Gerbil AVWTAPPVIFGWSRYWYFGLKTSVCGDFVSGTSPGVQSYMMVLMVTCIIFPLSIIIVLCYL
 Degu AVWTAPPVIFGWSRYWYFGLKTSVCGDFVSGTSPGVQSYMMVLMVTCIIFPLSIIIVLCYL
 Guinea AVWTAPPVIFGWSRYWYFGLKTSVCGDFVSGTSPGVQSYMMVLMVTCIIFPLSIIIVLCYL

IC3 **TM6**

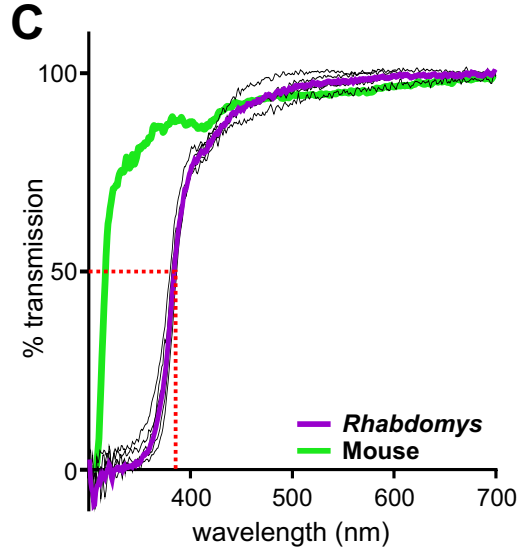
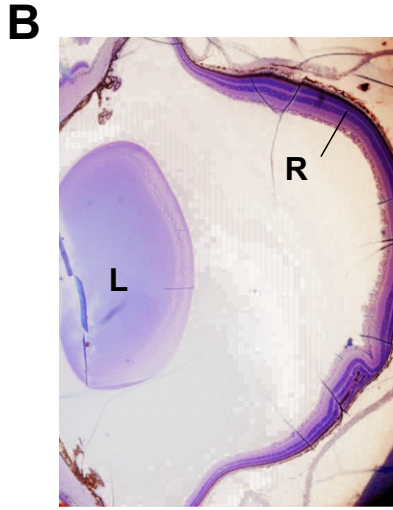
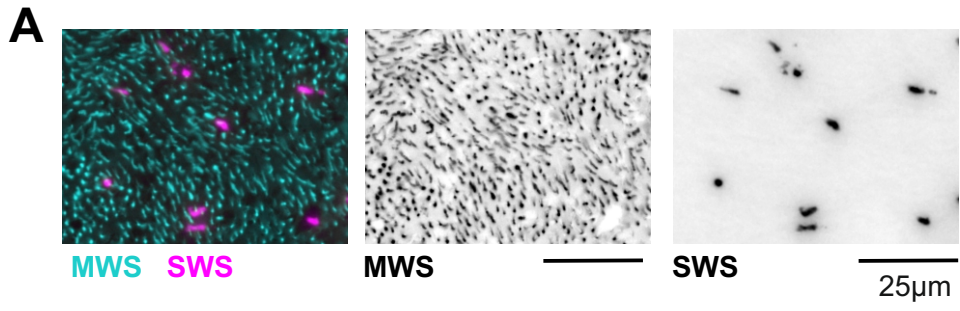
Rhabdo QVWLAI RAVAKQKQKESSTQKAEKEVTRMVMVVFAYCLCWGSPYVFFACFATAHPGYAFH 295
 Mouse QVWLAI RAVAKQKQKESSTQKAEKEVTRMVMVVFAYCLCWGSPYVFFACFATAHPGYAFH
 Rat QVWLAI RAVAKQKQKESSTQKAEKEVTRMVMVVFAYCLCWGSPYVFFACFATAHPGYAFH
 Gerbil QVWLAI RAVAKQKQKESSTQKAEKEVTRMVMVVFAYCLCWGSPYVFFACFATAHPGYAFH
 Degu HWWLAI RAVAKQKQKESSTQKAEKEVTRMVMVVFAYCLCWGSPYVFFACFATAHPGYAFH
 Guinea HWWLAI RAVAKQKQKESSTQKAEKEVTRMVMVVFAYCLCWGSPYVFFACFATAHPGYAFH

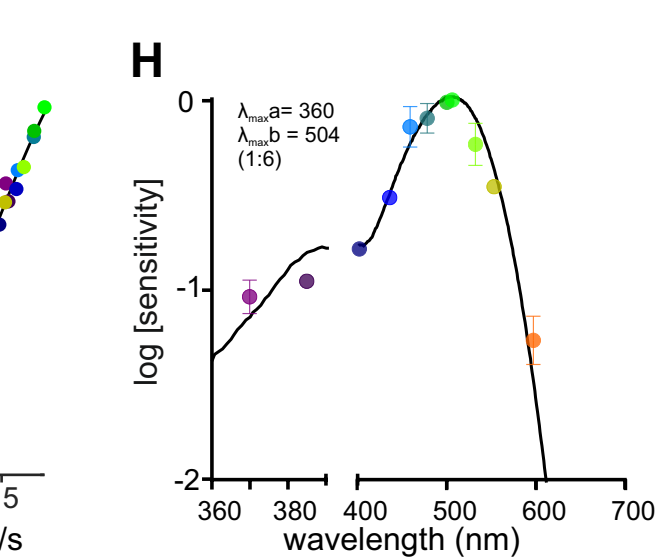
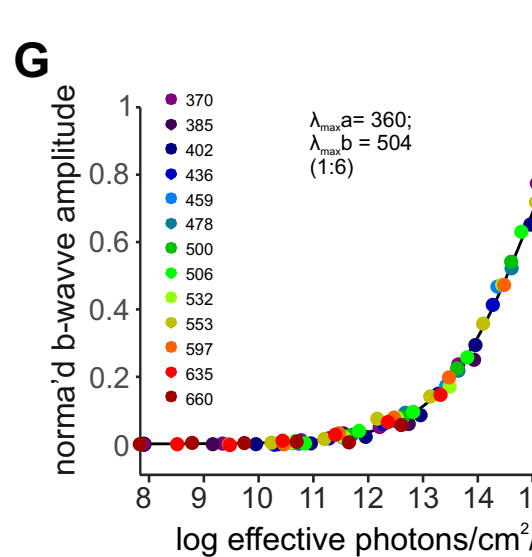
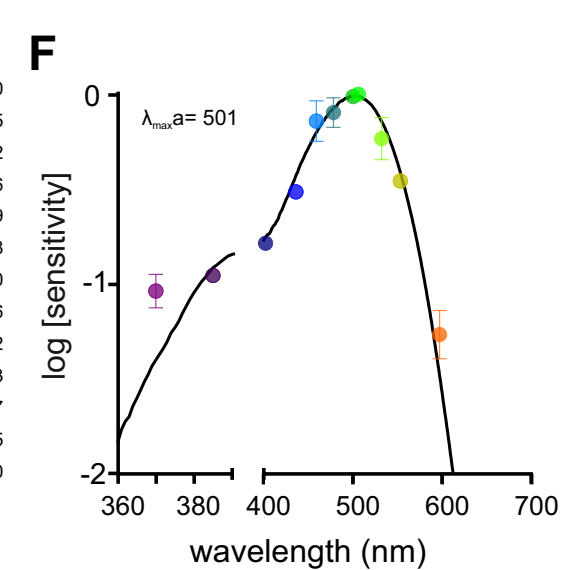
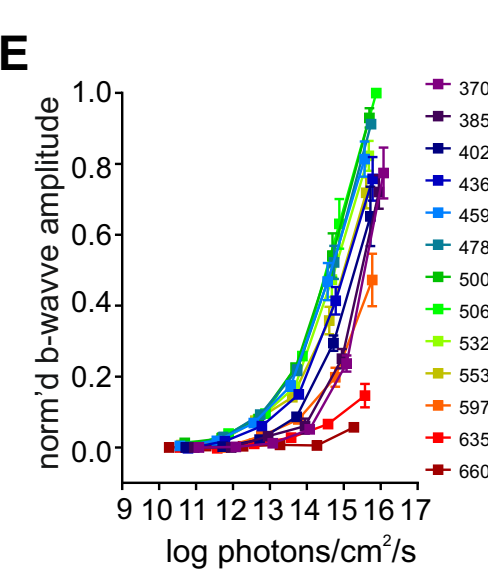
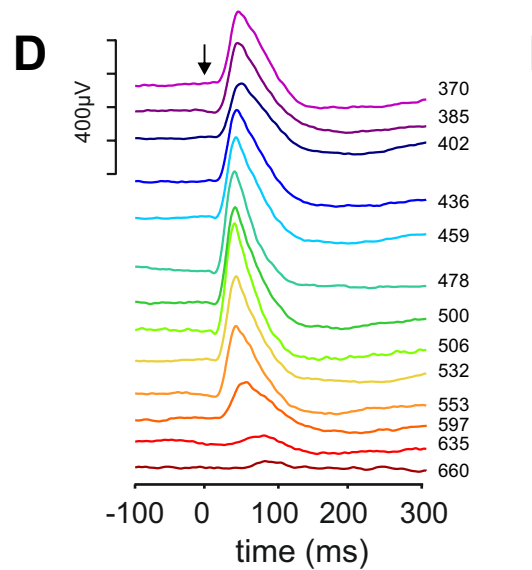
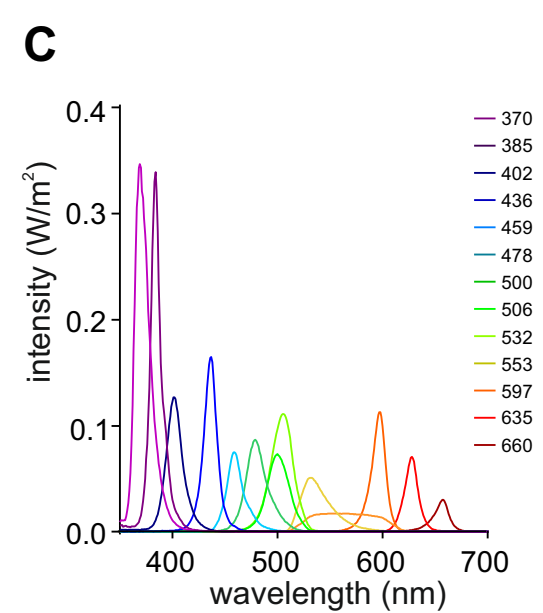
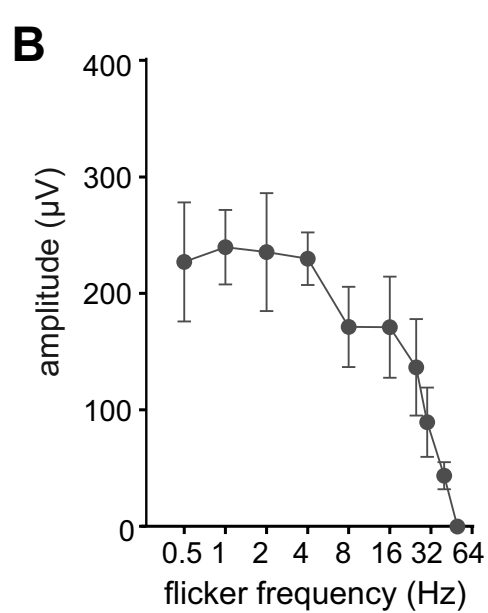
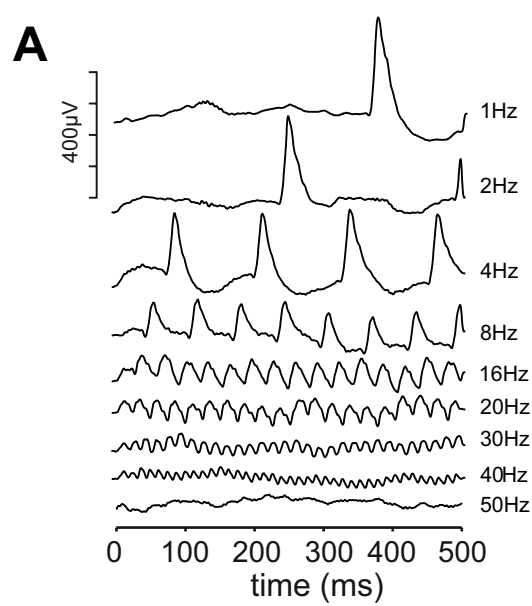
TM7 **C-terminus**

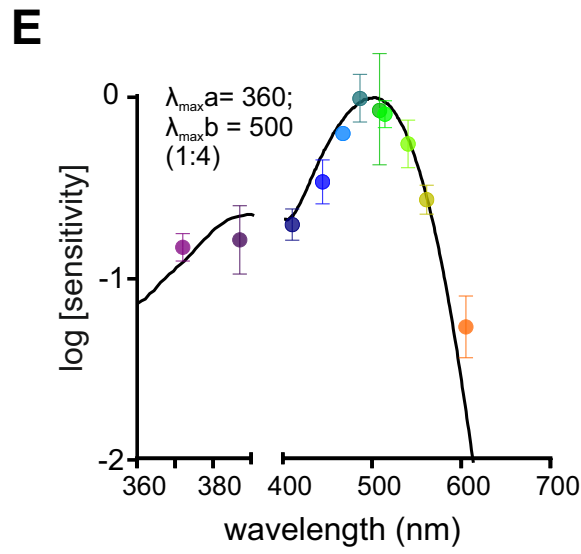
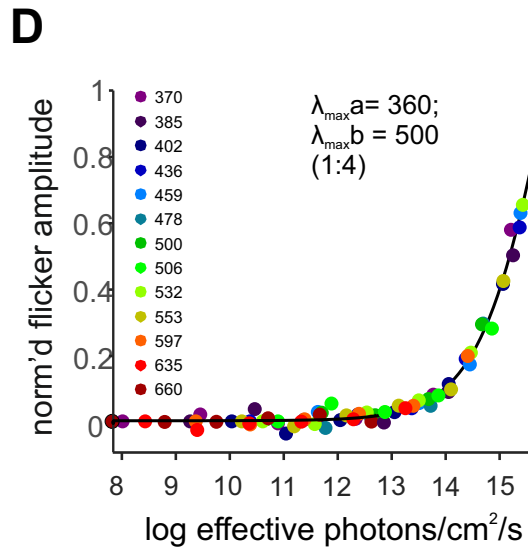
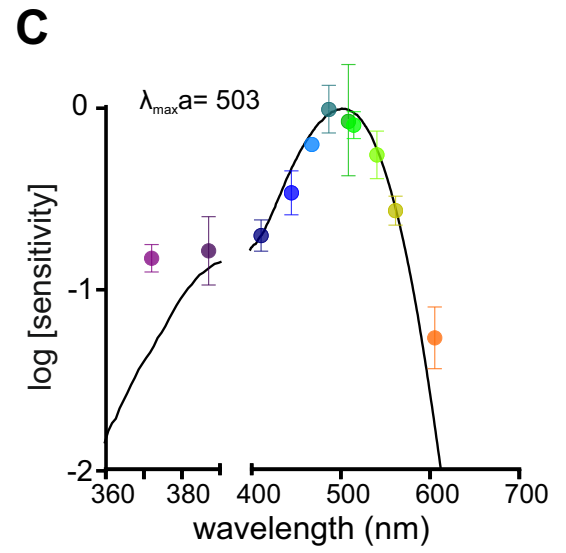
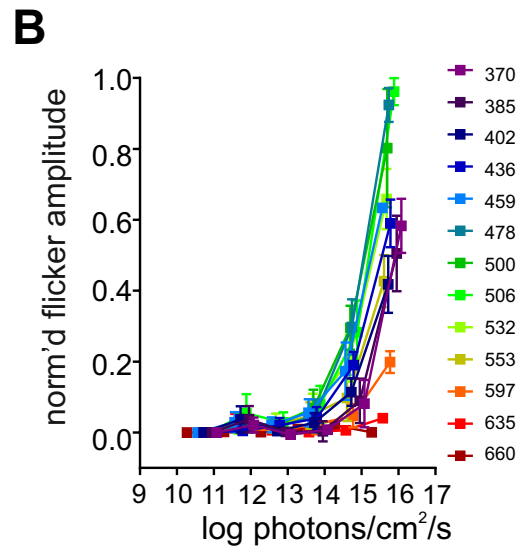
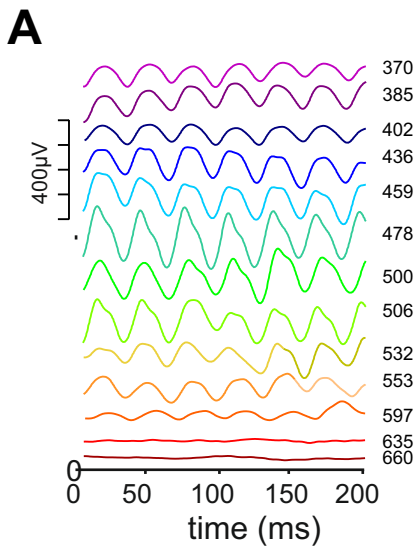
Rhabdo PLVASIPSPVFAKSAIYNPIIYVFMNRQFRNCILQLFGKVKVDDSSSELSTSKTEVSSVSS 353
 Mouse PLVASIPSPVFAKSAIYNPIIYVFMNRQFRNCILQLFGKVKVDDSSSELSTSKTEVSSVSS
 Rat PLVASIPSPVFAKSAIYNPIIYVFMNRQFRNCILQLFGKVKVDDSSSELSTSKTEVSSVSS
 Gerbil PLVASIPSPVFAKSAIYNPIIYVFMNRQFRNCILQLFGKVKVDDSSSELSTSKTEVSSVSS
 Degu PLVAALPSPVFAKSAIYNPIIYVFMNRQFRNCILQLFGKVKVDDSSSELSTSKTEVSSVSS
 Guinea PLVAALPSPVFAKSAIYNPIIYVFMNRQFRNCILQLFGKVKVDDSSSELSTSKTEVSSVSS

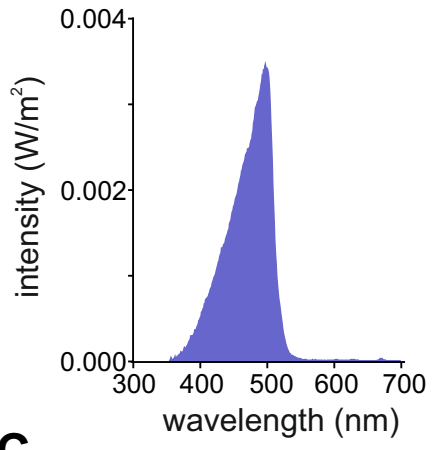
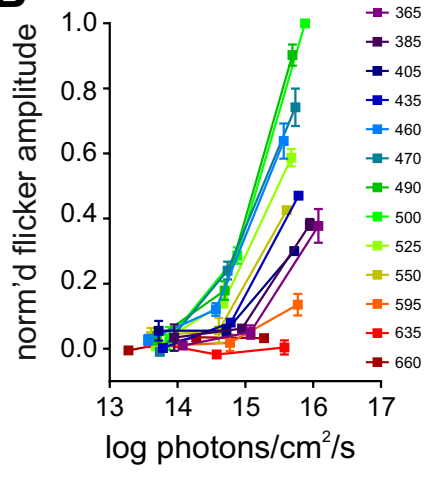
Site 292 Retinal Binding Site

Rhabdo VSPK 359
 Mouse VSPA
 Rat VSPA
 Gerbil VSPA
 Degu VSPA
 Guinea VSPA







A**B****C**